Analysis of the experimental spectral coherence in the Nysted Wind Farm

A. Vigueras-Rodríguez[1*)], Poul E. Sørensen[2)], Antonio Viedma[1)], Nicolaos A. Cutululis[2)], M. H. Donovan[3)]
[1)] Universidad Politécnica de Cartagena, 30203 Cartagena (Murcia), Spain
[*)] tlf. +34 968 32 5994, e-mail avigueras.rodriguez@upct.es
[2)] Risø DTU, VEA-118, P.O. Box 49, DK-4000 Roskilde, Denmark
[3)] DONG Energy, Copenhagen, Denmark

Abstract – In this paper, it is analysed the coherence between wind speeds located in a horizontal plane corresponding to hub height of wind turbines in a large wind farm.

The coherence is calculated through real data from Nysted Offshore Wind Farm. Concretely, the wind speed measured in the 72 Wind Turbines and in 2 of the meteorological masts during 9 months. The results are analysed in the scale of power fluctuations in large offshore wind farms.

This analysis shows the needing of a new spectral coherence model.

Index Terms – wind models, wind coherence, power fluctuation, offshore wind farms

1. INTRODUCTION

Nowadays the concern about the effects of the pollution (like the global warming effect) and the knowledge of the limitations of the fossil resources are creating a strong tendency in Europe towards the use of renewable energy sources. Therefore, there has been a big growth in the Wind Energy development, and it is expected to go on rising. Such growth makes essential to research deeply into this energy technology from the point of view of an important component of the electrical system, instead of considering only the local voltage quality as it was done previously [1].

A major issue in the control and stability of electric power systems is to maintain the balance between generated and consumed power. Because of the fluctuating nature of wind speeds, the increasing use of wind turbines for power generation has risen the interest in the fluctuations of the wind turbines power production, especially when the wind turbines are concentrated geographically in large wind farms. That fluctuation can also be a security issue in the future for systems with weak interconnections like Ireland or the Iberian Peninsula.

As example of the significance of these power fluctuations in Energinet.dk (the Danish Transmission System Operator), according to [2], Energinet.dk has observed that power fluctuations from the 160 MW offshore wind farm Horns Rev in West Denmark introduce several challenges to reliable operation of the power system in West Denmark. And also, that it contributes to deviations from the planned power exchange with the Central European Power System (UCTE). Moreover, it was observed that the time scale of the power fluctuations was from tens of minutes to several hours.

And in those fluctuations the importance of the spatial correlation of the wind speed in that time frame is shown by the fact that the power fluctuations of the 160 MW Wind Farm was significantly greater than the fluctuations in a similar capacity of Wind Turbines (WTs) distributed in smaller onshore Wind Farms. Those conclusions point out that the research of the spatial correlation is a main topic for the power fluctuation analysis.

In this way, models of coherence have been used within the modelling of wind farms regarding power fluctuation. [3] developed a wind speed model for a wind farm using a coherence model. In this case, the aim is to simulate the fluctuations in the shorter time scales related with the power quality characteristics.

Later on, an overall model for power fluctuations regarding the "long term" fluctuations described above has been developed [4].

2. COHERENCE MODELS

The spectral coherence between the wind speed in two different points is defined by

$$\gamma(f) = \frac{S_{ab}(f)}{\sqrt{S_{aa}(f)S_{bb}(f)}} \tag{1}$$

where $S_{ab}(f)$ is the crossed power spectral density (CPSD) between the wind speed in points a and b, and $S_{aa}(f)$ and $S_{bb}(f)$ are the power spectral density (PSD) of the wind in each point.

Besides the practical observation of the link between the power fluctuation and the spectral coherence above cited, different theoretical and practical observations have appeared in recent papers [5, 4] confirming that the seeking of power fluctuations models is totally linked with the coherence models in a wind farm frame.

Regarding the current coherence models, most of them are based in modifications to the Davenport model [6]. Davenport's model suggest an exponential behaviour explained by the following expression

$$|\gamma| = e^{-a\frac{d\cdot f}{V}} \tag{2}$$

where a, that is usually called decay factor, is a constant.

This model does not explain the inflow angle dependence, and so the usual modifications of this model, based in changing the value of the constant a have the same problem when using them in the scale of a wind farm, where this dependence is essential [7].

Nevertheless, the modifications suggested by [8] introduced that dependency expressing a as a function of the inflow angle

$$a = \sqrt{(a_{long}\cdot\cos\alpha)^2 + (a_{lat}\cdot\sin\alpha)^2} \tag{3}$$

being a_{long} and a_{lat} respectively the decay factors for the longitudinal and the lateral situations given by

$$a_{long} = (15 \pm 5)\cdot\frac{\sigma_v}{\bar{V}} \tag{4}$$

$$a_{lat} = (17.5 \pm 5)(m/s)^{-1}\cdot\sigma_v \tag{5}$$

being I_V the turbulent intensity defined by $I_V = \frac{\sigma_v}{\bar{V}}$

However, this empirical model was based on a very limited distance scale and so it does not predict the behaviour in the large wind farms of nowadays [7], so none of the usual models used in Wind Energy suits for studying the Power Fluctuation of Wind Farms. Therefore, in this paper the spectral coherence within a large wind farm is studied.

3. EXPERIMENTAL PROCEDURE OF THE COHERENCE MEASURING

The data used in this work is based in the Nysted Wind Farm, which is an offshore Wind Farm compound of 72 Siemens SWT-2.3-82 fixed speed wind turbines, with a global nominal power of 165.6 MW and distances between the wind turbines between 0.48 km and 7.73 km.

In the 72 WTs and the 2 Meteorological Masts shown in the figures, it has been measured the wind speed in the nacelle of each WT (69 m above ground), the active power produced, the yaw angle, the angular velocity and other variables. Furthermore, we have accesed to the wind speed and wind direction data from the meteorological masts at 70 m. above ground.

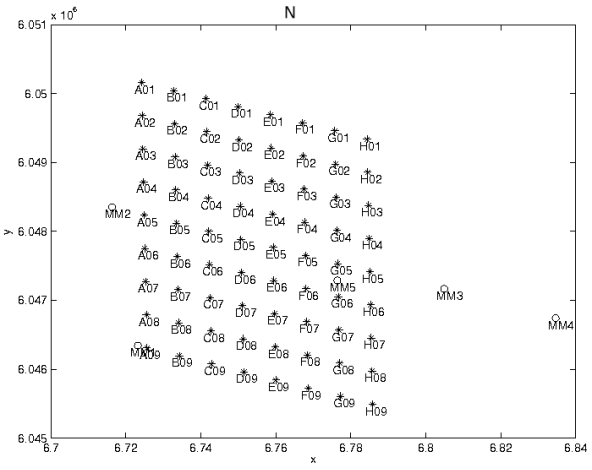

Figure 1. Layout of the Nysted Wind Farm

All of those data have been obtained through a SCADA system used by the wind farm main controller, which logs the data with a 1 Hz sampling frequency.

The data stored that have been used for this work is basically the wind speeds measured by each WT and the velocity and direction of the wind measured in the masts MM2 and MM3 that are shown in the figure 1, corresponding to 9 months in 2005.

All of this data is being processed in 2 hour intervals, so that coherence data is in a suitable time frame for this purpose.

Next, it has been selected only intervals with a 75% of valid data in MM_2 and MM_3. For the single Wind Turbine data a filtering for each Wind Turbine working in a "normal" state has been done by selecting the WTs with at least a 90% of valid data and holes smaller than 3 seconds, so that they can be fulfilled using splines without having any significant influence to the time scale that we are studying.

Then, it has been define similar pairs of WTs with similar distances and angles like A_{01}-A_{02} and C_{03}-C_{04}, calling them segments.

Following this process, as it is shown in figure 3, we consider all segments with more than 8 couples, as example some of those segments are shown in the table 1.

Once having selected the intervals, the data in each time interval are processed, averaging the power spectra of each couple of WTs belonging to the same segment.

For instance, when we consider the segment n compound of m pairs (being $m \geq 8$) of WTs with valid data (a_i, b_i), regarding the convolution property of the Fourier Transform:

$$S_{aa} = \frac{\sum_{i=1}^{m} \mathbf{FFT}(V_{a_i}) \cdot \mathbf{FFT}(V_{a_i})^*}{m} \quad (6)$$

$$S_{bb} = \frac{\sum_{i=1}^{m} \mathbf{FFT}(V_{b_i}) \cdot \mathbf{FFT}(V_{b_i})^*}{m} \quad (7)$$

$$S_{ab} = \frac{\sum_{i=1}^{m} \mathbf{FFT}(V_{a_i}) \cdot \mathbf{FFT}(V_{b_i}^*)}{m} \quad (8)$$

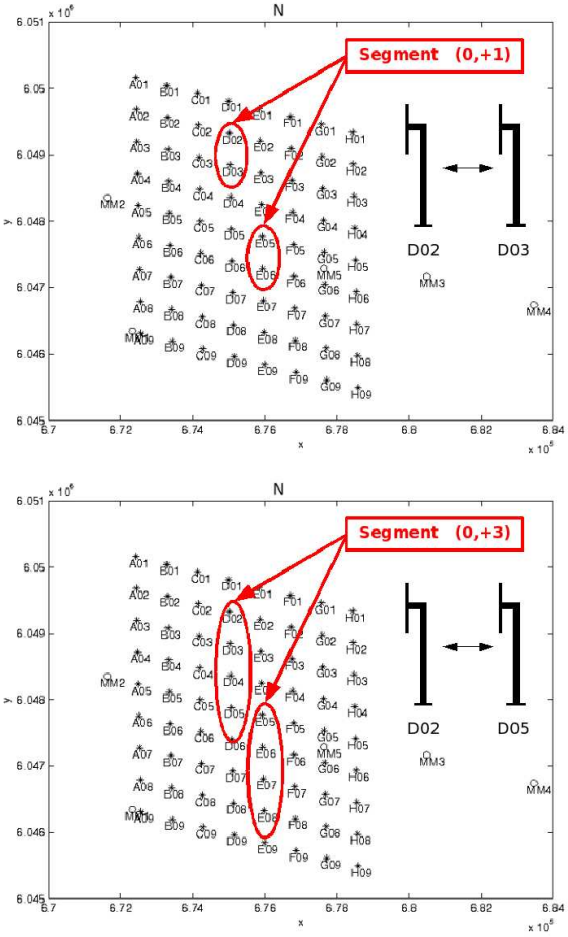

Figure 2. Example of how the segments are assembled.

where $S_{aa}(f), S_{bb}(f) \in \mathbb{R}$, as well as $S_{ab}(f) \in \mathbb{C}$. This is done for each segment with enough valid data in each time interval.

Afterwards, the results of each segment data $(S_{aa}(f), S_{bb}(f), S_{ab}(f))$ can be classified depending on the average wind speed $\overline{V}$ and the inflow angle α calculated through the segment angle β and the wind direction ϕ as shown in figure 3.

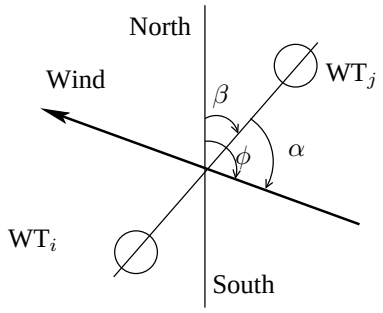

Figure 3. Definition of the inflow (α), segment (β) and wind direction angles (ϕ) used.

Next, the data classified for each segment (n) in the same wind speed range (v_m) and inflow angle range (α_k) are used for calculating the coherence $\gamma(n, v_m, \alpha_k, f)$ as follows:

$$\gamma(n, v_m, \alpha_k, f) = \frac{\sum_{i=1}^{N_n} S_{ab}(i, f) \cdot N_i}{\sqrt{\sum_{i=1}^{N_n} S_{aa}(i, f) \cdot N_i \cdot \sum_{i=1}^{N_n} S_{aa}(i, f) \cdot N_i}} \quad (9)$$

where N_i are the number of pairs of WT series of data used previ-

Δi_{row}	Δi_{column}	d_{xy}(m)	β_{xy}(deg.)	Blocks
0	1	482	-2	64
0	2	964	-2	56
0	3	1445	-2	48
0	4	1927	-2	40
0	5	2409	-2	32
0	6	2890	-2	24
0	7	3372	-2	16
0	8	3854	-2	8
1	0	867	-82	63
1	1	1062	-56	56
1	2	1403	-40	49
1	3	1810	-30	42
1	4	2246	-25	35
1	5	2698	-21	28
1	6	3158	-18	21
1	7	3625	-16	14
⋮	⋮	⋮	⋮	⋮
6	0	5204	-82	18
6	1	5308	-77	16
6	2	5454	-72	14
6	3	5637	-68	12
6	4	5853	-63	10
6	5	6101	-59	8
7	0	6071	-82	9
7	1	6173	-78	8
1	-7	3334	13	14
⋮	⋮	⋮	⋮	⋮
6	-5	5343	71	8
6	-4	5227	76	10
6	-3	5154	82	12
6	-2	5126	87	14
6	-1	5142	-88	16
7	-1	6007	-87	8

Table 1. Example of the 2-point segment characteristics.

ously for calculating the power spectral functions, i.e. the number m in equations 6,7 and 8.

The following 5 inflow angle bins are used $[0, 6, 25, 65, 84, 90]$(deg.), whereas the ranges of wind speed are $2m/s$ intervals from $2m/s$ to $16m/s$.

Finally, using the distance of each segment $d(n)$, we get an experimental $\gamma(d, v_m, \alpha_k, f)$.

In this proceeding the wake has been neglected, that is possible because in most of the pairs consider where both measures are inside of the overall wake, that affects similarly to both series of data and so, it is removed by the definition of the coherence itself (eq. 1). On the other hand, in the cases where the influence of having measures out of the wake and measures in the deep wake could be greater, looking at the expression of power spectral density of the wind inside and out of the wake that is shown by [4], we see that it does not affect to the time scale which we are interested in.

4. RESULTS

As it has been explained previously we have a package of coherence data ($|\gamma(d, v_m, \alpha_k, f)|$ and its argument $\angle\gamma(d, v_m, \alpha_k, f)$), from which we focus mainly in the module part.

Looking into the data, it is found a clear exponential dependence between the coherence and either the frequency f or the dimensionless frequency $\frac{d \cdot f}{V}$, as it is shown in figure 4.

Although looking to the figure 5, where that exponential dependence is represented in 3 different situations, it is also shown that its decay factors are quite different on each situation, and therefore it is not realistic to fit them to a single decay factor.

Then, taking into account the inflow angle, we can focus firstly in the data corresponding to the longitudinal situation ($\alpha_1 \Rightarrow \alpha \in [0,\, 6\,\text{deg}]$) plotted in figure 6, where the decay factor a (see 2) is plotted for different wind speed ranges against the distance. In that figure, it is possible to see that there is not any significant tendency in the variation of that parameter with the distance or the wind speed ($a_{long} \neq f(d, V)$). Therefore, it is possible to assume that a constant value for the longitudinal situation a_{long} (see 4) would be suitable in this distance and time frame. This would agree qualitatively (but not quantitatively) to Schlez & Infield model (Eq. 3).

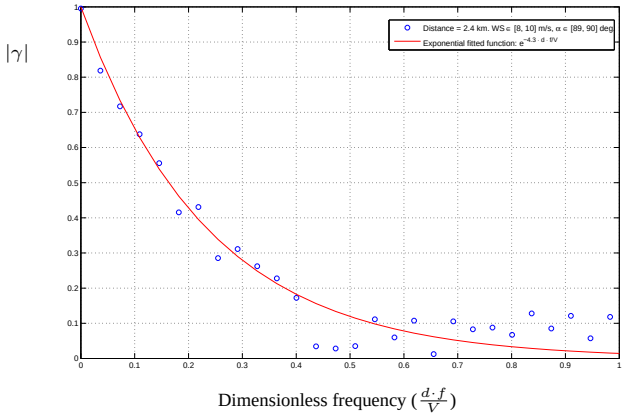

Figure 4. Coherence measured in Nysted Wind Farm in the longitudinal situation and an exponential curve fitted to the data.

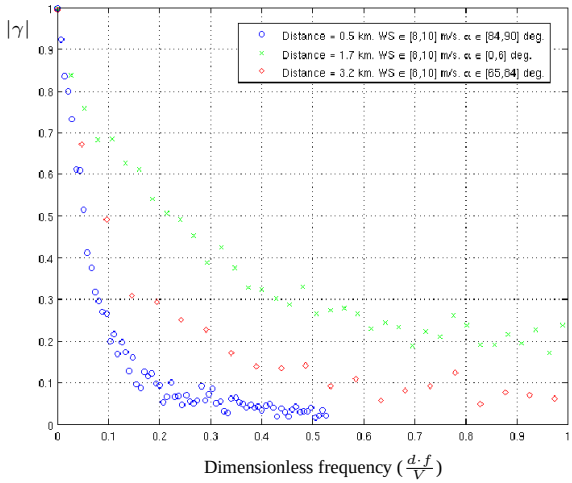

Figure 5. Coherence measured in Nysted Wind Farm in 3 different situations.

However, in the lateral situation ($\alpha_5 \Rightarrow \alpha \in [84,\, 90\,\text{deg}]$), the decay factor parameter depends significantly on the distance and the wind speed ($a_{lat} = f(d, V)$), as it is shown in figure 7 , and this was not predict by the Schlez & Infield model due to the different time and length scale in the distance between the points (100 m) and in the height above ground (18 m).

Looking into the figure, it is possible to see that a_{lat} gets lower when the distance rises, a_{lat} rises when wind speed gets greater, and those changes of a_{lat} get less significant as the distance gets greater.

Looking at the intermediate situations ($\alpha_2, \alpha_3, \alpha_4$), it is possible to see an intermediate behaviour between the longitudinal and the

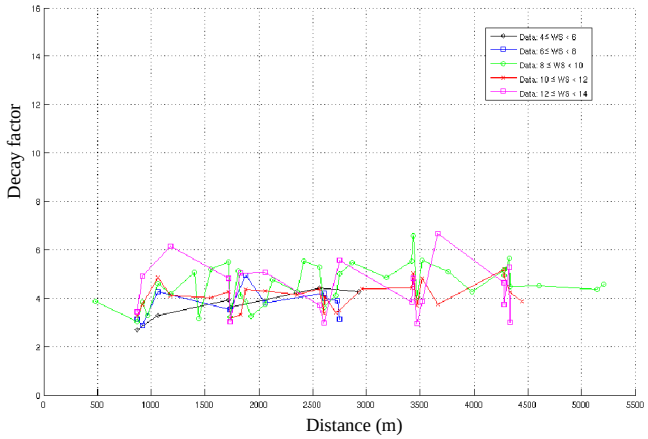

Figure 6. Decay factor of the coherence in the longitudinal situation.

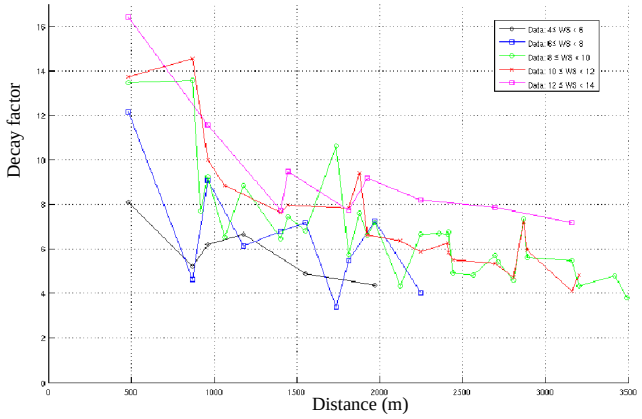

Figure 7. Decay factor of the coherence in the lateral situation.

lateral situation, as it was suggested by the Schlez & Infield model.

Therefore, the coherence can be considered explained by eq. 2, where the decay factor is a function $a = a(\alpha, d, V)$ complying the following conditions:

$$\alpha \to 0 \quad \Rightarrow \quad \Delta a(\Delta d, \Delta V) \to 0 \tag{10}$$

$$d \uparrow \quad \Rightarrow \quad a \downarrow \tag{11}$$

$$V \uparrow \quad \Rightarrow \quad a \uparrow \tag{12}$$

$$d \uparrow\uparrow \quad \Rightarrow \quad \Delta a(\Delta d, \Delta V) \downarrow \tag{13}$$

$$\alpha \downarrow \quad \Rightarrow \quad \Delta a(\Delta d, \Delta V) \downarrow \tag{14}$$

5. Conclusion

It has been processed 9 months of real data coming from a Large Offshore Wind Farm, selecting 2 hour intervals. In which the coherence have been calculated. It has been considered all the inflow angle situations and for the whole range of wind speed where the wind farm is working often, and with distances from near 0.5 km to 6 km.

It has been seen that there is a significant dependence between the coherence and the inflow angle, as in the model suggested by Schlez & Infield. However, it was also shown that in the length, height and time scale interesting for studying the power fluctuations of Large Wind Farms, the Schlez & Infield model predicts coherence values that are far from the experimental data shown here.

In those experimental data is shown that whereas the longitudinal situation ($\alpha \approx 0$) can be modelled by means of a constant decay factor, there is a strong dependency between the decay factor and the distance and wind speed, being this dependency stronger as the inflow angle gets closer to the lateral situation ($\alpha = \pi/2$).

This analysis has been generalised in a paper submitted to the Journal of Wind Engineering and Industrial Aerodynamics [9].

Acknowledgment

The work presented in this paper has been done in the research project "Power Fluctuations from large offshore wind farms" financed by the Danish Transmission System Operator Energinet.dk as PSO 2004 project number 6506.

A. Vigueras-Rodríguez is supported by the Spanish Ministerio de Educación y Ciencia through the grant program "Becas FPU" and from the national research project "ENE2006-15422-C02-02".

References

[1] P. Sørensen, N. A. Cutululis, T. Lund, A. D. Hansen, T. Sørensen, et al.: Power quality issues on wind power installations in Denmark, in IEEE Power Engineering Society, General Meeting, Tampa, Florida, USA.

[2] V. Akhmatov, J. P. Kjaergaard, H. Abildgaard: Announcement of the large offshore wind farm Horns Rev B and experience from prior projects in Denmark, in European Wind Energy Conference.

[3] P. Sørensen, A. D. Hansen, P. E. C. Rosas: Wind models for simulation of power fluctuations from wind farms, Journal of Wind Engineering and Industrial Aerodynamics vol. 90, 2002, pp. 1381–1402.

[4] P. Sørensen, N. Cutululis, A. Vigueras-Rodríguez, H. Madsen, P. Pinson, et al.: Modelling of power fluctuations from large offshore wind farms, Wind Energy .

[5] T. Nanahara, M. Asari, T. Sato, K. Yamaguchi, M. Shibata, et al.: Smoothing effects of distributed wind turbines. Part 1. Coherence and smoothing effects at a wind farm, Wind Energy vol. 7, 2004, pp. 61–74.

[6] A. G. Davenport: The spectrum of horizontal gustiness near the ground in high winds, Quarterly Journal of Meteorology Society vol. 87, no. 372, 1961, pp. 194–211.

[7] A. Vigueras-Rodríguez, P. Sørensen, A. Viedma: Spectral coherence models for the wind speed in large wind farms, in Proceedings of the 2nd PhD Seminar on Wind Energy in Europe, European Academy of Wind Energy, Roskilde (Denmark).

[8] W. Schlez, D. Infield: Horizontal, two point coherence for separations greater than the measurement height, Boundary-Layer Meteorology vol. 87, 1998, pp. 459–480.

[9] A. Vigueras-Rodríguez, P. Sørensen, A. Viedma, M. H. Donovan: Spectral coherence model for power fluctuations in a wind farm, submitted to Journal of Wind Engineering and Industrial Aerodynamics.